Copyright © 1991, by the author(s).
All rights reserved.

Permission to make digital or hard copies of all or part of this work for personal or classroom use is granted without fee provided that copies are not made or distributed for profit or commercial advantage and that copies bear this notice and the full citation on the first page. To copy otherwise, to republish, to post on servers or to redistribute to lists, requires prior specific permission.

ANALYSIS OF AN ELECTRON WAVE INTERFERENCE FILTER IN THE PRESENCE OF AN APPLIED ELECTRIC FIELD USING OPTICAL PLANE WAVE ANALOGIES

by

Julie A. Kenrow

Memorandum No. UCB/ERL M91/19

4 March 1991

ANALYSIS OF AN ELECTRON WAVE INTERFERENCE FILTER IN THE PRESENCE OF AN APPLIED ELECTRIC FIELD USING OPTICAL PLANE WAVE ANALOGIES

by

Julie A. Kenrow

Memorandum No. UCB/ERL M91/19

4 March 1991

ELECTRONICS RESEARCH LABORATORY

College of Engineering
University of California, Berkeley
94720

TITLE PAGE

ANALYSIS OF AN ELECTRON WAVE INTERFERENCE FILTER IN THE PRESENCE OF AN APPLIED ELECTRIC FIELD USING OPTICAL PLANE WAVE ANALOGIES

by

Julie A. Kenrow

Memorandum No. UCB/ERL M91/19

4 March 1991

ELECTRONICS RESEARCH LABORATORY

College of Engineering
University of California, Berkeley
94720

Abstract

Electron wave devices are becoming increasingly important as semiconductor growth techniques become more precise. In this paper the effect of an applied electric field on the transmission and bandwidth characteristics for a narrow band Fabry-Perot electron wave interference filter is investigated. The analysis of the electron wave filter is treated analogously to an electromagnetic wave filter, assuming ballistic electron behavior. The procedure for designing a superlattice interference filter is reviewed, and a numerical procedure is presented, demonstrating how to obtain the response of a superlattice filter when an applied electric field is present. Results of numerical calculations are presented, demonstrating filter passband response. Fundamental differences between electron waves and electromagetic waves are demonstrated and the differences between the filter reponses for each type of wave are explained.

I. Introduction

Recently, analogies between electromagnetic (EM) plane waves and quantum mechanical electron waves propagating in layered structures have been utilized to design electron wave devices such as low, high and bandpass filters and waveguides [1-4]. Such work has been motivated by the ongoing progress in semiconductor growth techniques, particularly in molecular-beam epitaxy (MBE) and metalorganic chemical vapor deposition (MOCVD). Currently these techniques enable the growth of multilayered semiconductor superlattice structures with precise monolayer composition control. Of particular interest are the growth of multi-quantum well structures (i.e. successively grown layers of narrow and wide band-gap materials). Such structures, grown with good quality materials (minimal crystalline structure imperfections) have great potential (1), for developing ballistic electron transport devices such as high speed

transistors and (2), for developing electron optics devices such as beamsplitters, lenses and diffraction gratings, required to control freespace electron beams for electron spectroscopy and electron diffraction analysis of crystals.

MBE grown superlattice structures typically range in thickness from several tens to several hundreds of angstroms and are typically grown with alternating layers of an alloy such as $Al_xGa_{1-x}As$ with different mole fractions x. Electron transport through such thin structures may be considered ballistic (collisionless) since the mean free path for scattering in these high quality crystals is typically on the order of 0.1 μm or more [5]. Recently, ballistic or near-ballistic transport has been demonstrated across device widths ranging from 300-5000 Å [6]. The assumption of collisionless transport greatly simplifies the analysis of electron motion through superlattices, since the solution of the Schrödinger equation yields plane wave behavior.

Gaylord et al. have demonstrated that such electron waves exhibit many of the properties of EM plane waves, such as reflection, refraction, interference and diffraction [1]. Hence, the solution of electron transport through a multilayered quantum well structure proceeds in a manner completely analogous to the transmission of light through multi-layer thin film dielectrics. Gaylord et al. have utilized this analogy to study the design of both electron-wave slab waveguides and superlattice interference filters [2-4]. In particular, they have presented design procedures for a narrow passband Fabry-Perot filter and have calculated cut-off frequencies and propagating modes for electron wave guiding structures. For both devices, the analysis was simplified by considering only normal incidence of a single electron, thereby ignoring the effects of a realistic distribution of incident electron kinetic energies and angles. In addition, for both devices it was assumed that no applied electric field was present.

The potential importance of these new electron wave devices for a wide variety of applications suggests that further studies need to be carried out that consider effects such as incident electron distribution functions, applied electric fields and quantum mechanical tunneling. The purpose of this paper is to investigate the effects on the transmission and bandwidth characteristics for a narrow band Fabry-Perot electron wave interference filter in the presence of an applied electric field. In section II, the basic analogies between EM and electron plane wave propagation are reviewed. Next, in section III the design of a superlattice interference filter is reviewed, and a numerical procedure is presented, demonstrating how to obtain the response of a superlattice filter when an applied electric field is present. In section IV, results of numerical calculations are presented, demonstrating filter passband response. Finally, in section V, conclusions are drawn and suggestions are made for further studies.

II. Comparison of EM and Electron Plane Wave Properties

The transmission and reflection characteristics of optical EM plane waves at a boundary between dielectrics is well known. For a transverse electric (TE) polarized wave incident at angle θ_i, with wavenumber $k = 2\pi n/\lambda_o$ on a boundary (see Fig. 1), the transmissivity and reflectivity are given by

$$t_o = \frac{2n_1\cos\theta_i}{n_1\cos\theta_i + n_2\cos\theta_t} \tag{1}$$

$$r_o = \frac{n_1\cos\theta_i - n_2\cos\theta_t}{n_1\cos\theta_i + n_2\cos\theta_t} \tag{2}$$

where n is the index of refraction and λ_o is the freespace wavelength. These results can easily be extended to a system of M dielectric layers, such that for the ith layer,

$$t_{oi} = \frac{2n_i\cos\theta_{i_i}}{n_i\cos\theta_{i_i} + n_{i+1}\cos\theta_{t_i}} \tag{3}$$

$$r_{oi} = \frac{n_i\cos\theta_{i_i} - n_{i+1}\cos\theta_{t_i}}{n_i\cos\theta_{i_i} + n_{i+1}\cos\theta_{t_i}} \tag{4}$$

Finally, the overall reflectivity and transmissivity can be obtained by simple 2x2 matrix multiplication, yielding

$$\begin{bmatrix} 1 \\ E_{r,0} \end{bmatrix} = \prod_{i=1}^{M} \frac{1}{t_{o,i}} \begin{bmatrix} 1 & r_{o,i} \\ r_{o,i} & 1 \end{bmatrix} \begin{bmatrix} \exp(jk_{o,i}d_i\cos\theta_i) & 0 \\ 0 & \exp(-jk_{o,i}d_i\cos\theta_i) \end{bmatrix} \mathrm{x}$$
$$\frac{1}{t_{o,M+1}} \begin{bmatrix} 1 & r_{o,M+1} \\ r_{o,M+1} & 1 \end{bmatrix} \begin{bmatrix} \psi_{t,M+1} \\ 1 \end{bmatrix} \tag{5}$$

where E is the electric field amplitude.

The analogous results for an electron plane wave incident at angle θ_i, with wavenumber $k_i = [2m_i^*(W-V_i)]^{1/2}/\hbar$ incident on the $(i+1)$th potential barrier/well of a superlattice structure (see Fig. 2) are given by

$$t_{ei} = \frac{2[(W-V_i)/m_i^*]^{1/2}\cos\theta_{i_i}}{D} \tag{6}$$

$$r_{ei} = \frac{[(W-V_i)/m_i^*]^{1/2}\cos\theta_{i_i} - [(W-V_{i+1})/m_{i+1}^*]^{1/2}\cos\theta_{t_i}}{D} \tag{7}$$

where

$$D = [(W-V_i)/m_i^*]^{1/2}\cos\theta_{i_i} + [(W-V_{i+1})/m_{i+1}^*]^{1/2}\cos\theta_{t_i}$$

and [2],

$$\begin{bmatrix} 1 \\ \psi_{r,0} \end{bmatrix} = \prod_{i=1}^{M} \frac{1}{t_{e,i}} \begin{bmatrix} 1 & r_{e,i} \\ r_{e,i} & 1 \end{bmatrix} \begin{bmatrix} \exp(jk_{e,i}d_i\cos\theta_i) & 0 \\ 0 & \exp(-jk_{e,i}d_i\cos\theta_i) \end{bmatrix} \text{x}$$

$$\frac{1}{t_{e,M+1}} \begin{bmatrix} 1 & r_{e,M+1} \\ r_{e,M+1} & 1 \end{bmatrix} \begin{bmatrix} \psi_{t,M+1} \\ 1 \end{bmatrix} \tag{8}$$

where ψ is the electron wavefunction, m_i^* is the electron effective mass for the ith layer, V_i is the conduction band potential energy for the ith layer and W is the total electron energy. Upon comparison of (3)-(5) and (6)-(8), analogous quantities for TE polarized EM waves and electron waves are

$$E \Leftrightarrow \psi$$

$$n \Leftrightarrow \sqrt{(W-V_i)/m_i^*} \qquad \text{for amplitude calculations}$$

$$\Leftrightarrow \sqrt{(W-V_i)m_i^*} \qquad \text{for phase calculations}$$

A similar analysis can be performed for TM polarized EM waves.

III. Superlattice Interference Filter with Applied Electric Field

Before considering the addition of an applied field, a brief outline of the design procedure for electron wave interference filters will be presented [2]. Consider the specific case of a Fabry-Perot filter [8] with the form $[HL]^4HH[LH]^4$, to be designed here using $Al_xGa_{1-x}As$ as the semiconductor superlattice material. For the EM case, H and L refer to high and low refractive index, respectively, whereas for the electron wave

case, H and L refer to the low and high mole fraction x, respectively. An illustration of this device can be seen in Fig. 3.

The required high and low mole fractions are determined for a specified incident pass kinetic energy $W - V_o$, by simultaneously requiring the thickness of each layer to be an integral multiple of the monolayer thickness and requiring the thicknesses to be odd multiples of a quarter wavelength as measured in each region. Application of these requirements results in the following solution for the compositions x_i,

$$x_i = [-\mathrm{b} + (b^2 - 4ac_i)^{1/2}]/2a, \tag{9}$$

where

$$a = AC, \quad b = AB - CW_o,$$
$$c_i = (h^2/32m_o)[(2q_i - 1)^2/p_i^2 r_i^2] - BW_o,$$
$$p_i, q_i = 0, 1, 2, \ldots,$$

r_i is the monolayer thickness, and A, B and C are material constants that describe the variation of the conduction band edge (referenced to GaAs) and electron conduction band effective mass with x_i as follows,

$$V_i = Ax_i \tag{10}$$
$$m_i^* = (B + Cx_i)m_o. \tag{11}$$

Values for x_i are determined by looping through values of p_i and q_i until, for a particular q_i, two or more solutions of x_i are found, corresponding to different values of p_i, such that $0 \leq x_i \leq 0.45$. This range of x_i represents usable compositions of $Al_xGa_{1-x}As$ for use as a direct band-gap material.

As an illustration, consider the following numerical example. For the device shown in Fig. 3, let the pass kinetic energy be 0.2 eV and let $x_o=x_{M+1}=0.45$. For $Al_xGa_{1-x}As$ grown along the [100] direction, the monolayer thickness is 2.83 Å, independent of material composition. Furthermore, for $Al_xGa_{1-x}As$, $A=0.773$ [2], $B=0.067$, and $C=0.083$ [9]. For these values, $V_o=0.348$ eV, $W=0.548$ eV and the solution of (9) yields the two roots, $x_1=0.204$ and $x_2=0.397$, for $p_1=6$ and $p_2=7$ and $q=1$. The corresponding thicknesses of the two layers are given by $d_1=p_1r_1=16.9$ Å and $d_2=p_2r_2=19.8$ Å. It should be noted that other solutions may exist for larger values of q, but for practical purposes, solutions for the smallest possible value of q are desired, since this leads to the smallest possible layer thicknesses. It is also of importance to point out that for this example, the values obtained for x_1 and x_2 in [2] are slightly in error. Coincidentally or not, their resulting transmissivity plot yields the "expected" result, i.e., centered on the design pass kinetic energy and symmetric about this kinetic energy, analogous to the corresponding Fabry-Perot optical filter. Transmissivity results presented in section IV indicate somewhat different results. The implications of these discrepancies will be discussed further in section IV.

Consider now the analysis of a semiconductor superlattice structure in the presence of an applied electric field. In principle, the exact solution of the Schrödinger wave equation for a multi-quantum well structure with an applied electric field is quite difficult to obtain. However, it will be demonstrated here that a simple extension of (8) leads to a simple numerical solution of the Schrödinger equation.

An applied voltage across a superlattice structure such as that of Fig. 3 results in tilting of the energy bands as shown in Fig. 4. In each layer, the magnitude of the electric field is constant, hence the conduction band edge varies linearly with distance. A simple approximation involves a staircase model for the band edge, as illustrated in

Fig. 4 [10]. With this approximation, an equivalent problem can now be considered in which each layer is treated consisting of many sub-layers. While each sub-layer will retain the same effective mass, each will have a different kinetic energy, $W-V_{ij}$, corresponding to the jth sub-layer of the ith superlattice layer. Hence, (8) can be solved for the equivalent problem with MxN layers, where M is the number of real internal layers and N is the number of sub-layers into which each real layer is divided.

The details for obtaining the sub-layer V_{ij} values is straightforward. For a given applied voltage V_a, the following set of equations, obtained from elementary electrostatics considerations,

$$\epsilon_i E_i = \epsilon_{i+1} E_{i+1} \qquad \text{for } i=1, 2, \ldots, M-1 \tag{12}$$

$$\sum_{i=1}^{M} E_i d_i = V_a \tag{13}$$

can be solved to obtain an expression for E_1,

$$E_1 = V_a \left[d_1 + \sum_{i=2}^{M} (\epsilon_{i-1} d_i / \epsilon_i) \right]^{-1} \tag{14}$$

from which all the electric fields in the other layers can be found through use of (12). Finally, the sub-layer V_{ij} values can be found from knowledge of the electric fields in each layer as follows,

$$V_{ij} = V_o + \sum_{k=1}^{i-1} E_k d_k + (j d_i / N) E_i \tag{15}$$

As a numerical illustration, consider the filter characteristics specified previously

and now consider an applied voltage V_a=0.1 volts. The static dielectric constant for each layer, required in (12), is given by [9]

$$\epsilon_i = 13.18 - 3.12x_i, \tag{16}$$

and solution of (12)-(14) yields E_1=30.4 kV/cm and E_2=31.9 kV/cm. The actual transmission charactistic for this filter will be presented in section IV. As a practical point, it should be possible in the laboratory to apply a voltage entirely across the internal layers of a semiconductor superlattice structure. If the end layers of the structure are highly doped and then contacted to metal leads, the voltage V_a should drop only across the undoped or lightly doped internal layers.

IV. Numerical Results and Discussion

Transmission characteristics for the Fabry-Perot interference electron wave filter design presented in the previous section have been computed for several pass kinetic energies and values of applied voltage. The transmission response T for the filter is obtained from the relation

$$T = 1 - R = 1 - |r_{eT}|^2$$

where r_{eT} is the overall reflectivity of the filter, i.e., $r_{eT} = \psi_{t,M+1}/1$, which can directly be obtained from (8).

In Fig. 5 the transmission is plotted for filter designs of 0.1, 0.2 and 0.3 eV pass kinetic energies and V_a=0. The FWHM bandwidth is seen to vary with the designed pass kinetic energy (KE_o), and equals 1.3 meV for the 0.1 eV curve, 11 meV for the 0.2 eV curve and 5.3 meV for the 0.3 eV curve. Though not visible on the resolution of

Fig. 5, the actual pass kinetic energy (where T=1), for each curve deviates slightly from the designed value. The transmission peaks computed were shifted 0.53%, 0.44% and 0.38% below the designed values of 0.1, 0.2 and 0.3 eV, respectively. The relative significance of these shifts in KE_o are related to the bandwidths resulting from each design. For example, for the 0.1 eV curve, a shift of 0.53% in the pass kinetic energy should be considered significant since it represents a shift nearly out of the passband. In contrast, for the 0.2 eV curve, a shift of 0.44% in KE_o represents a shift only 8% as great as the bandwidth. These results suggest that it may be necessary in some cases to iterate the design procedure a few times to obtain a filter response that is within the tolerance of the design specifications. This inherent limitation was not observed in [2]. In fact, in that work it was claimed that the actual pass kinetic energy coincides exactly with the design value. Also, as Fig. 5 illustrates, the actual transmission is not exactly symmetrical about the pass kinetic energy. This again is in contrast with [2], where it is claimed that the response is identical to the corresponding symmetrical EM Fabry-Perot filter response. The somewhat asymmetrical responses in Fig. 5 are physically reasonable and are a direct result of the correspondence principle of quantum mechanics. That is, as the incident kinetic energy is increased further and further above the highest conduction band edge, the electron behaves more and more like a classical particle, and in the high kinetic energy limit, it shouldn't even "see" the quantum well structure. Thus, the increasingly classical behavior of the electron, as the kinetic energy is increased above KE_o, should lead to the observed nature of the asymmetry in Fig. 5.

In Figs 6-8, the transmission for several values of both positive and negative applied voltage is plotted for KE_o= 0.1, 0.2 and 0.3 eV. With increasing $V_a > 0$ (see Fig. 4), the transmission peaks shift upward in kinetic energy, the bandwidth decreases

and the peak transmission values decrease. In contrast, for $V_a < 0$ and $|V_a|$ increasing, the transmission shifts downward in kinetic energy, the bandwidth increases and the peak transmission values decrease, but only slightly. All of the above deviations from the corresponding $V_a=0$ curves will significantly alter the filter response and thus when designing narrow passband electron filters, the influence of an applied electric field which is of practical importance, must be taken into consideration. At present, a systematic design procedure, incorporating the effect of an applied voltage does not exist. However, an iterative design procedure, similar to that discussed in the previous section can be implemented.

The qualitative behavior of the filter response to an applied electric field in Figs 6-8 is easily explained by quantum mechanical considerations. Note that for incident electron kinetic energies less than the applied voltage, the transmission equals zero, corresponding to the complete reflection of the electron wave. The broadening or narrowing of the transmission curves and the decrease in peak value are due to two distinct effects. First, application of any applied voltage, resulting in a tilted conduction band edge will result in some deviation from the original filter design for $V_a=0$. Second, the applied field, depending on the sign of V_a, will either accelerate or decelerate the electron as it traverses the filter, hence should aid electron transmission for $V_a < 0$ and hinder electron transmission for $V_a > 0$. This effect is mainly evident upon comparison of the respective bandwidths for corresponding values of $\pm V_a$. For $V_a<0$, the bandwidth broadening is a result of the accelerating field, which tends to partially cancel the filtering out of electrons with incident kinetic energies disparate from the pass kinetic energy. In contrast, for $V_a > 0$, the bandwidth narrowing is a result of the decelerating field, which generally impedes electron transmission.

V. Conclusions

The analysis of an electron wave Fabry-Perot interference filter in the presence of an electric field has been presented. The close analogy between the optical multilayer thin film dielectric structure and the semiconductor multi-quantum well structure, demonstrated in previous work, has been used to obtain the transmissivity and reflectivity of the semiconductor superlattice structure. Using these expressions, a simple numerical procedure was implemented to obtain a solution to the Schrödinger wave equation which includes the effect of an applied voltage. It was demonstrated that physically reasonable applied voltages significantly alters the passband response. In particular, an applied voltage $V_a > 0$ ($V_a < 0$) lowered the peak value of the transmission, shifted the pass kinetic energy downward (upward) and decreased (increased) the FWHM bandwidth.

The slight shift in pass kinetic energy and asymmetrical passband transmission response obtained from this study indicates that further investigation needs to be carried out to fully understand the complete relationship between optical plane waves and electron plane waves. Furthermore, a systematic study needs to be carried out to investigate generally the effect of applied fields for all electron wave devices, which as has been demonstrated here, can be quite significant. A more complete model of electron transport through quantum well structures should also include a distribution of initial electron kinetic energies and momenta, as well as electron-electron interactions.

References

[1] T. K. Gaylord and K. F. Brennan, "Electron wave optics in semiconductors," *J. Appl. Phys.*, vol. 65, pp. 814-820, 1989.

[2] T. K. Gaylord, E. N. Glytsis, and K. F. Brennan, "Semiconductor superlattice interference filter design," *J. Appl. Phys.*, vol. 65, pp. 2535-2540, 1989.

[3] T. K. Gaylord, E. N. Glytsis, and K. F. Brennan, "Semiconductor quantum wells as electron wave slab waveguides," *J. Appl. Phys.*, vol. 66, pp. 1842-1848, 1989.

[4] T. K. Gaylord, E. N. Glytsis, and K. F. Brennan, "Semiconductor electron-wave slab waveguides," *J. Appl. Phys.*, vol. 66, pp. 1483-1485, 1989.

[5] R. A. Stewart, private communication.

[6] Srinivasan Krishnamurthy, M. A. Berding, A. Sher, and A.-B. Chen, "Ballistic transport in semiconductor alloys," *J. Appl. Phys.*, vol. 63, pp. 4540-4547, 1988.

[7] Ajoy K. Ghatak, K. Thyagarajan, and M. R. Shenoy, "Numerical Analysis of Planar Optical Waveguides Using Matrix Approach," *J. Lightwave Technol.*, vol. LT-5, pp. 660-667, 1987.

[8] H. A. Macleod, *Thin-Film Optical Filters*. New York: Macmillan, 1986.

[9] Sadao Adachi, "GaAs, AlAs, and $Al_xGa_{1-x}As$: Material parameters for use in research and device applications," *J. Appl. Phys.*, vol. 58, pp. R1-R29, 1985.

[10] Ajoy K. Ghatak, K. Thyagarajan, and M. R. Shenoy, "A Novel Numerical Technique for Solving the One-Dimensional Schroedinger Equation Using Matrix Approach—Application to Quantum Well Structures," *IEEE J. Quantum Electron.*, vol. 24, pp. 1524-1530, 1988.

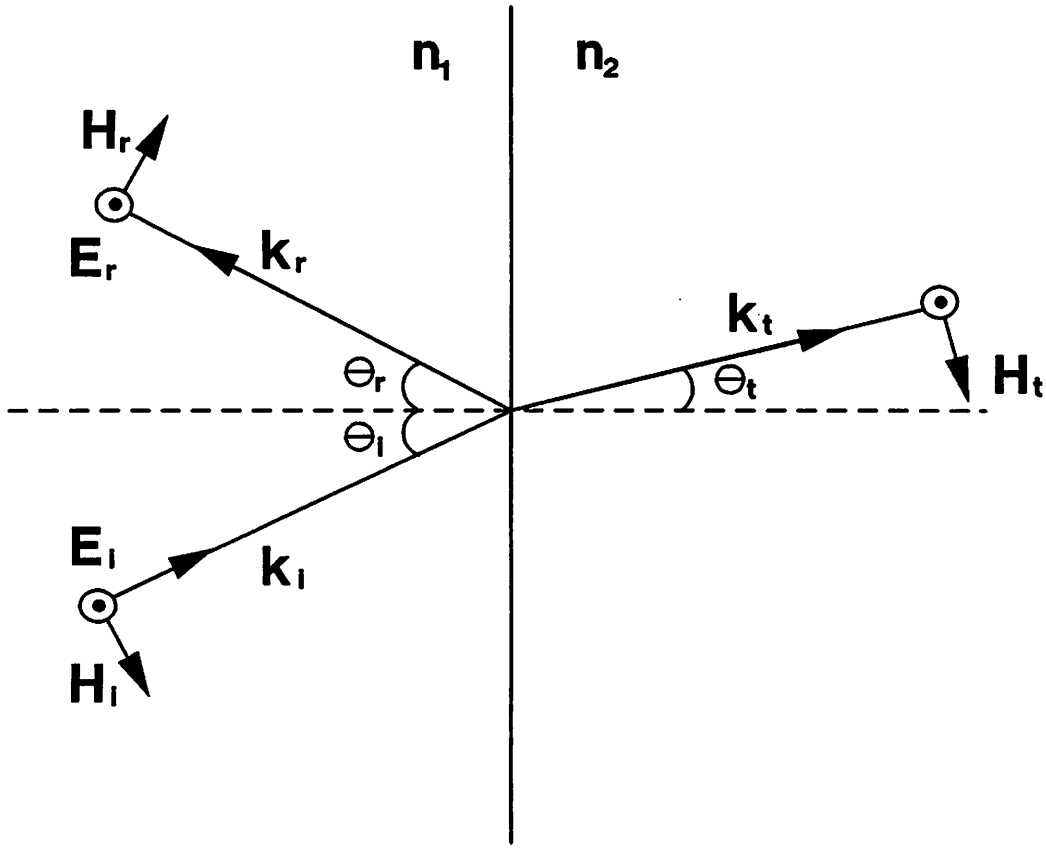

Figure 1. TE plane wave incident at angle θ_i on a dielectric interface.

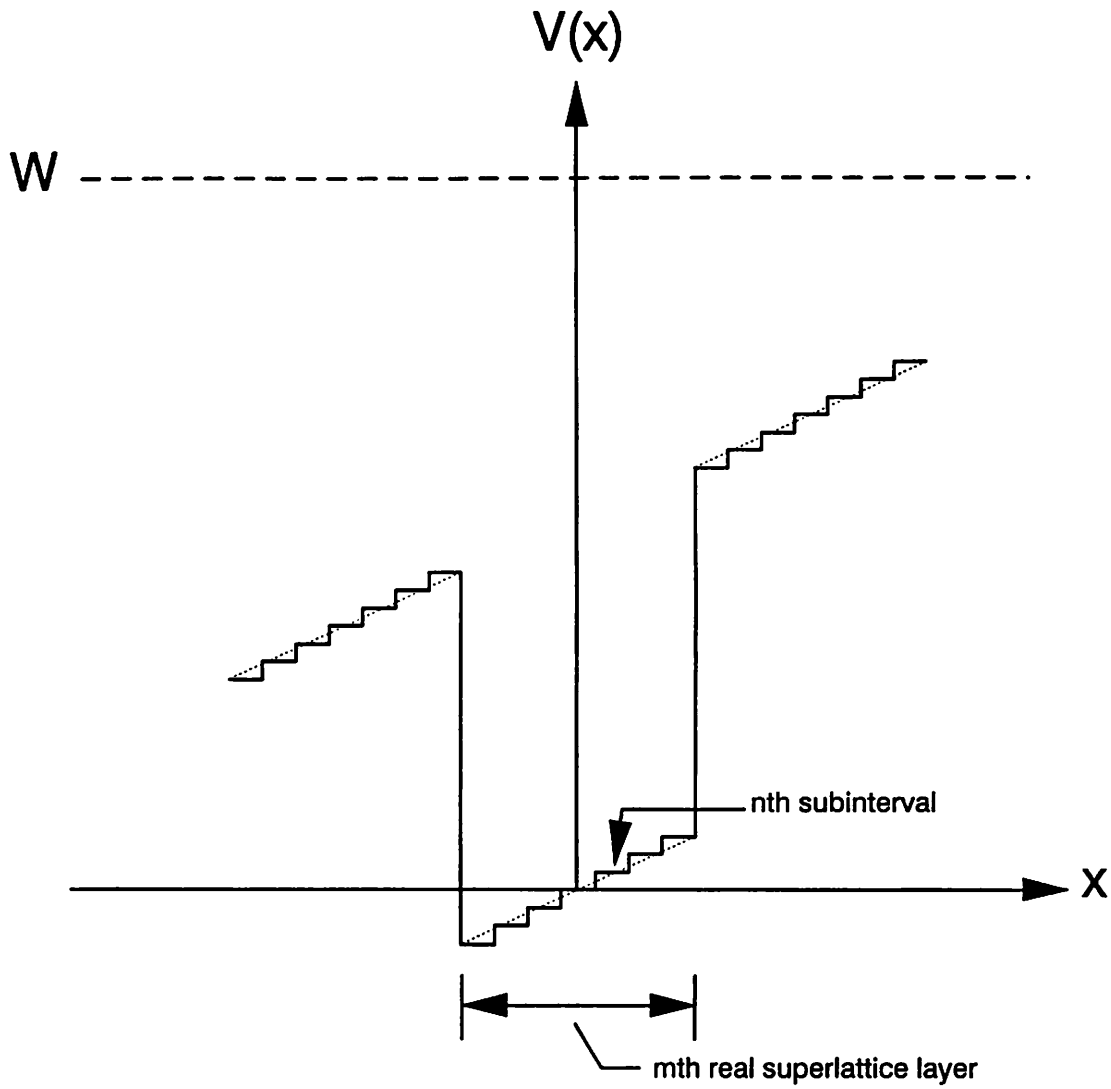

Figure 4. A single quantum well in the presence of an applied electric field and the corresponding staircase approximation for dividing the mth well/barrier region into N subintervals. Note that the electron energy is greater than the altered barrier potentials in order for transport to occur.

Figure 5. Transmission $|\psi_t/\psi_i|^2$ versus incident kinetic energy for pass kinetic energies of 0.1, 0.2 and 0.3 eV.

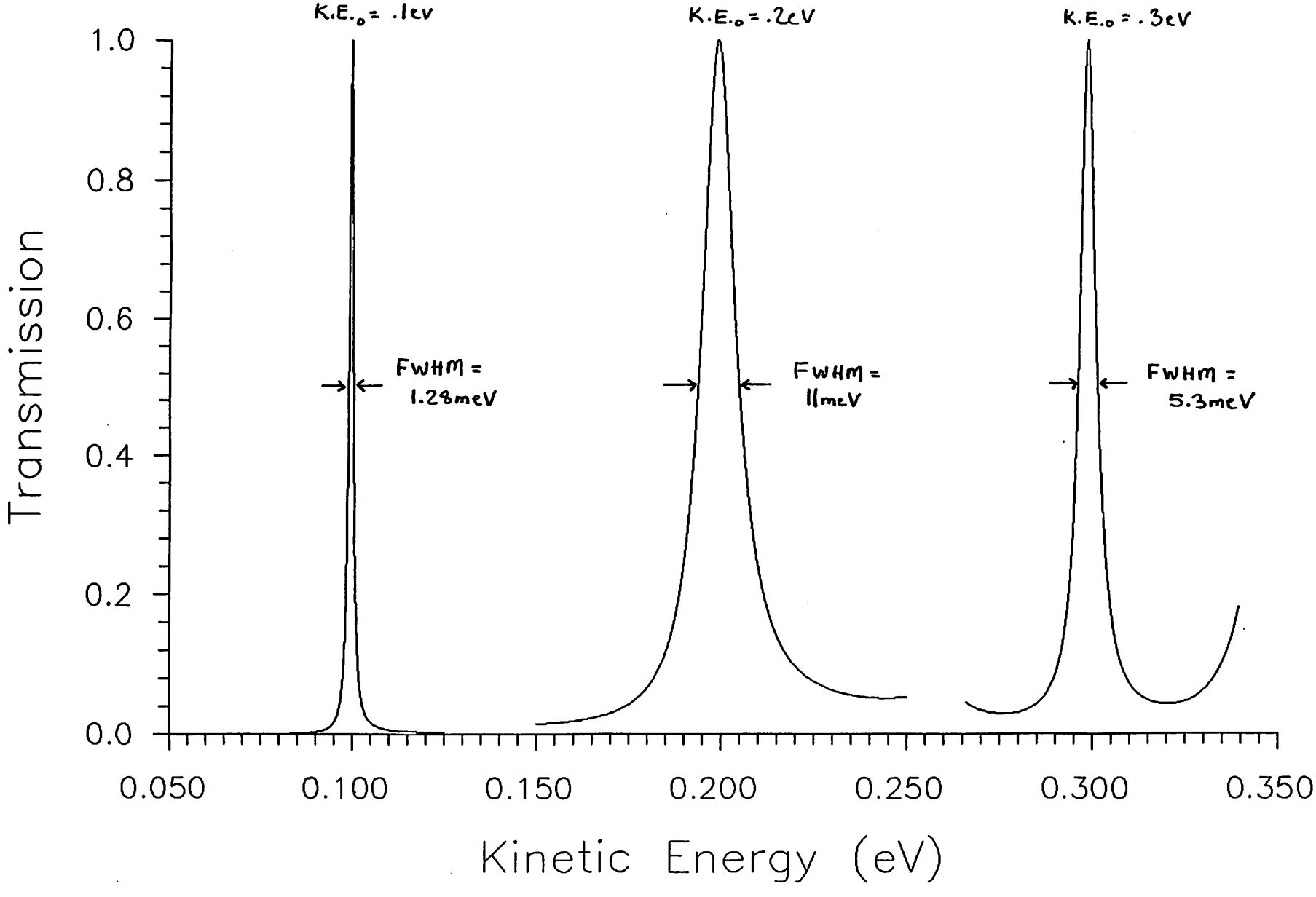

Figure 6. Fabry-Perot filter passband response for K.E.$_o$=0.1 eV with applied voltages V_a=−0.1, −0.05, 0, 0.05, 0.075, 0.09, and 0.1 volts.

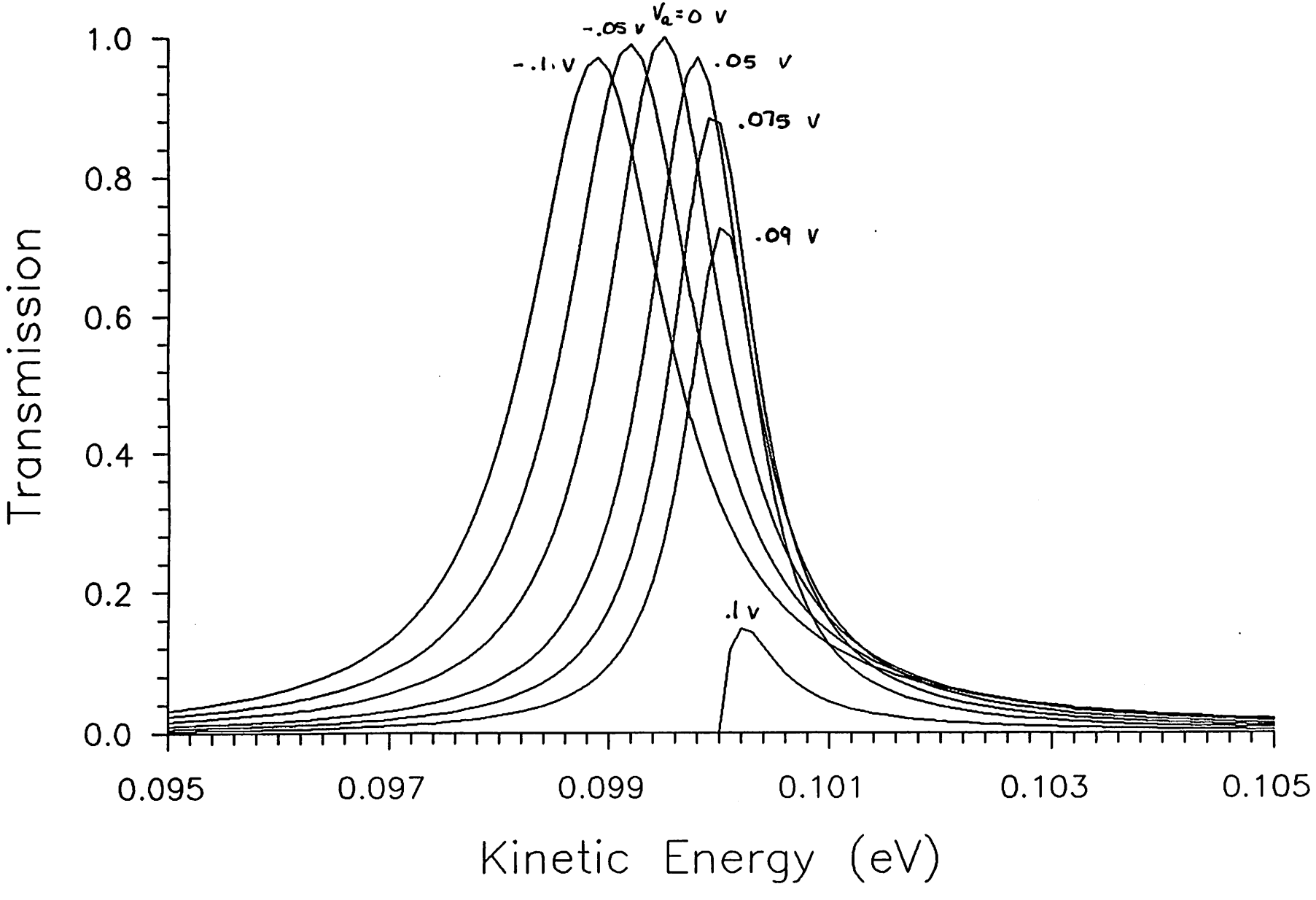

Figure 7. Fabry-Perot filter passband response for K.E.$_o$=0.2 eV with applied voltages V_a=−0.3, −0.2, −0.1, 0, 0.1, 0.175, 0.19, and 0.2 volts.

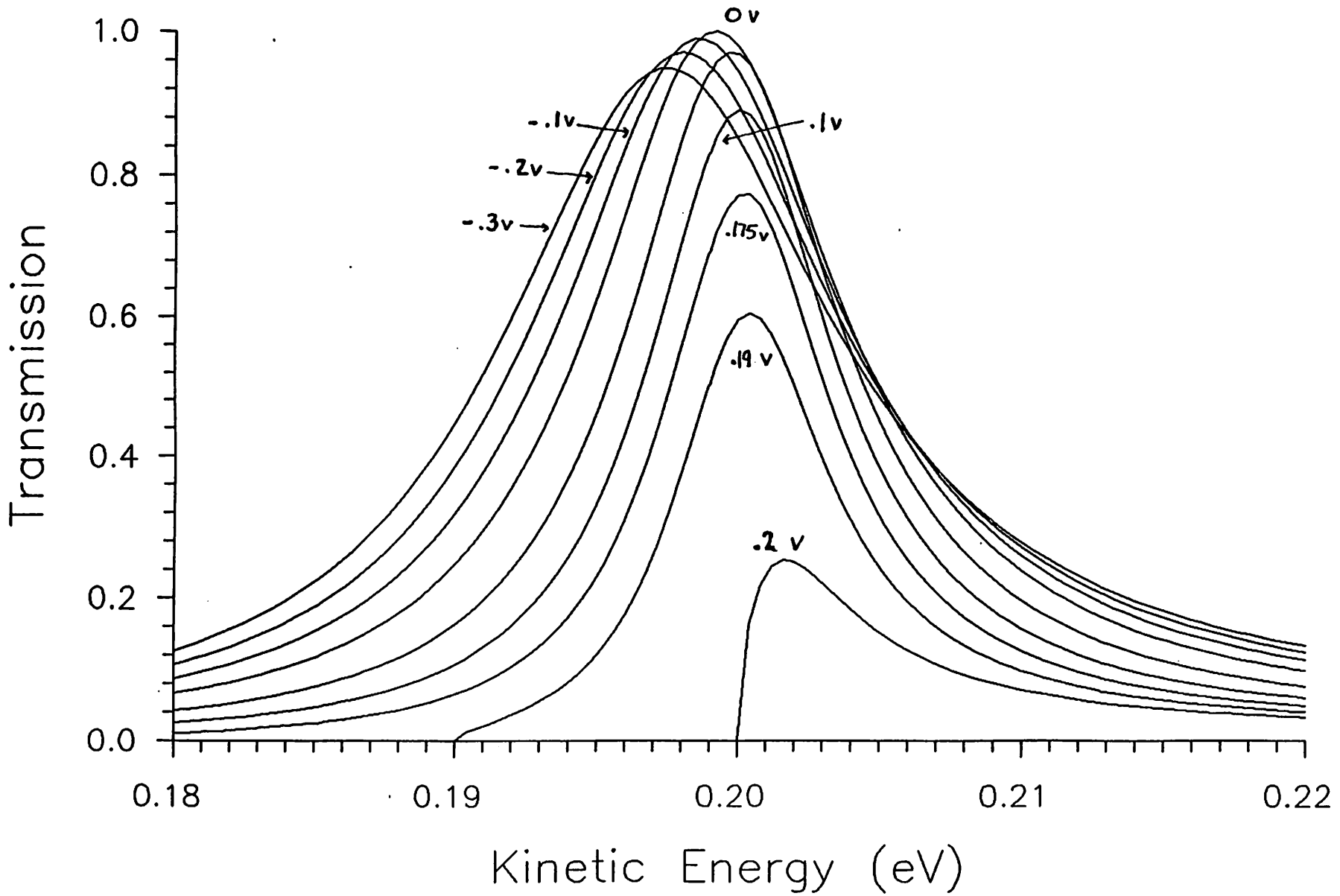

Figure 8. Fabry-Perot filter passband response for K.E.$_o$=0.3 eV with applied voltages V_a=−0.25, −0.1, 0, 0.1, 0.2, 0.25, and 0.3 volts.